

# Exosome Derived from Mesenchymal Stem Cells Alleviates Hypertrophic Scar by Inhibiting the Fibroblasts via TNFSF-13/HSPG2 Signaling Pathway

Huimin Zhang<sup>1,\*</sup>, Chengyu Zang<sup>1,2,\*</sup>, Wen Zhao<sup>1</sup>, Linfeng Zhang<sup>1</sup>, Rui Liu<sup>1</sup>, Zhang Feng<sup>1</sup>, Jie Wu<sup>1</sup>, Rongtao Cui<sup>1-3</sup>

<sup>1</sup>Department of Burn and Plastic Surgery, Shandong Provincial Hospital Affiliated to Shandong First Medical University, Jinan, People's Republic of China; <sup>2</sup>Department of Burn and Plastic Surgery, Shandong Provincial Hospital, Shandong University, Jinan, People's Republic of China; <sup>3</sup>Medical Science and Technology Innovation Center, Shandong First Medical University & Shandong Academy of Medical Sciences, Jinan, People's Republic of China

\*These authors contributed equally to this work

Correspondence: Rongtao Cui, Department of Burn and Plastic Surgery, Shandong Provincial Hospital Affiliated to Shandong First Medical University, Jinan, People's Republic of China, Tel +86 18653170822, Email cuirt1986@outlook.com

**Background:** Mesenchymal stem cell-derived exosomes (MSC-exo) have been shown to have significant potential in wound healing and scar relief processes. According to reports, TNFSF13 and HSPG2 are associated with various fibrotic diseases. The aim of this study is to investigate how TNFSF13 and HSPG2 affect the formation of hypertrophic scar (HS) and the mechanism by which exosomes regulate HS.

**Methods:** Immunohistochemistry, qRT-PCR, Western blot, and immunofluorescence were performed to measure TNFSF13 expression in HS skin tissues and hypertrophic scar fibroblast (HSF). HSF were treated with recombinant TNFSF13 protein and TNFSF13 siRNAs to probe the effect of TNFSF13 on the activity of HSF. The CCK-8, EdU, Transwell, and Western blot were used to investigate the role of TNFSF13 in viability, proliferation and inflammation. The influence of MSC-exo on the proliferation and function of HSF was determined by scratch and Western blot.

**Results:** TNFSF13 was dramatically up-regulated in HS skin tissues and HSF. Recombinant TNFSF13 protein increased cell viability, proliferation, migration, fibrosis, inflammation, and the binding between TNFSF13 and HSPG2 of HSF. The opposite results were obtained in TNFSF13 siRNAs transferred HSF. Furthermore, TNFSF13 activated the nuclear factor- $\kappa$ B (NF- $\kappa$ B) signaling pathway. Silencing of HSPG2 and inhibition of NF- $\kappa$ B remarkably eliminated the promoting effects of TNFSF13 on cell viability, proliferation, migration, fibrosis and inflammation of HSF. MSC-exo reduced  $\alpha$ -SMA and COL1A1 inhibited the proliferation and migration of HSF by inhibiting TNFSF13 and HSPG2.

**Conclusion:** TNFSF13 activates NF- $\kappa$ B signaling pathway by interacting with HSPG2, which regulates the proliferation, migration, fibrosis and inflammatory response of HSF. Through the above mechanisms, knocking out TNFSF13 can inhibit the proliferation, migration, fibrosis and inflammatory response of HSF, whereas MSC-exo could reverse this process. These results suggest that MSC-exo alleviates HS by inhibiting the fibroblasts via TNFSF-13/HSPG2 signaling pathway.

**Keywords:** TNFSF13, HSPG2, hypertrophic scar(HS), MSC-exo, fibroblasts

## Introduction

Hypertrophic scar (HS) is a fibroproliferative disease caused by abnormal skin tissue repair after burns, lacerations, and surgical trauma.<sup>1-3</sup> It is currently believed that wound repair is a complex dynamic process in which multiple repair cells, growth factors and extracellular matrix interact, in which fibroblasts play a pivotal role.<sup>4</sup> Fibroblasts fill tissue defects by

proliferating, synthesizing and secreting a large amount of ECM. However, under the action of certain cytokines, excessive proliferation and secretion of fibroblasts lead to abnormal deposition of ECM, which can form HS.<sup>5</sup> HS are often accompanied by erythema, bumps, itching, and pain, leading to organ dysfunction and motor loss at different degrees, making HS an increasingly serious social health problem.<sup>6–8</sup> Currently, the treatment for HS includes surgical excision, laser therapy, radiation therapy, pressure therapy and medication. The surgical incision is an invasive procedure that may result in new scarring,<sup>9–11</sup> and intradermal injection is usually accompanied by adverse reactions. However, the results remain unsatisfactory due to individual differences.<sup>12</sup> Thus, it is important to investigate the pathogenesis of HS and search new therapeutic strategies for HS.

Mesenchymal stem cells (MSC), a type of pluripotent stem cell, can self-renew and differentiate into other cells. The characteristics make them widely used in tissue engineering and regenerative medicine.<sup>13</sup> Despite the advantages of MSC, their clinical application has resulted in a variety of side effects, including immune response, short life, neoplasm formation, obstruction of small vessels, low homing properties, and ethical issues.<sup>14</sup> Exosomes (EXOs) are the smallest extracellular vesicles,<sup>15</sup> just 30–150 nm in diameter, contain protein, mRNA, microRNA and other biological information.<sup>16</sup> They are found in biological fluids such as milk, saliva, urine, semen, serum, bile, lymph, plasma, amniotic fluid, and cerebrospinal fluid.<sup>17,18</sup> MSC are the principal sources from which EXOs are isolated.<sup>15</sup> Owing to no immune rejection, greater stability, no tumorigenesis, no vascular obstruction, and an intrinsic homing property, EXOs have enormous potential as desirable drug/gene delivery vectors in the field of disease treatment and tissue repair.<sup>19</sup> Recently, significant contributions to wound healing and scar attenuation through exosome derived from mesenchymal stem cells (MSC-exo) have been described. Some researchers confirmed that MSC-Exo has anti-inflammatory and immunomodulatory properties and can be used for inflammatory diseases, skin injuries, and skin scar formation.<sup>20,21</sup> H. Kim et al showed that exosomes derived from alternatively activated M2 Mφs can promote cutaneous wound repair.<sup>22</sup> Wang et al reported in diabetic mice, exosomes from adipose-derived stem cells promoted collagen deposition, which increased in the late stage of wound healing.<sup>23</sup> In our study, we attempted to further reveal the effect of MSC-exo on HS.

TNFSF13 (a member of the tumor necrosis factor superfamily 13), also known as the A proliferation-inducing ligand (APRIL), is a type II transmembrane protein composed of a short N-terminal, variable-length transmembrane region, and an extracellular C-terminal in the cell.<sup>24</sup> It is a trimeric protein, and its precursor is secreted into the cytoplasm after cleavage by furin protease. As a ligand for TNFRSF17/BCMA, TNFSF13 has been found to be important for B cell development, autoimmunity, and cancer. TNFSF13 was also found to be a potential fibrogenic molecule and involved in fibroblast recruitment of macrophages. In spinal cord injury (SCI), TNFSF13 gene deletion reduced the area of fibrosis scar.<sup>25</sup> So we speculate that TNFSF13 may play a role in regulating the formation and development of HS.

HSPG2, encoded by HSPG2 gene, is a major component of vascular basal membrane.<sup>26</sup> A recent report suggested HSPG2 on target cell surfaces can act as receptors for exosome uptake.<sup>27</sup> Other studies have showed that HSPG2 is associated with several fibrotic processes, such as liver fibrosis and connective tissue proliferative tumors.<sup>28,29</sup> Shu et al found that HSPG2 deficient mice showed decreased production of TGF- $\beta$  in mouse skin.<sup>30</sup> In addition, the targeted binding of HSPG2 to TNFSF13 is involved in regulating atherosclerosis.<sup>31</sup> However, as for the association of HSPG2 and TNFSF13 with exosomes, it remains unclear.

In our previous research, we confirmed exosomes have potential in the field of scar alleviation: MSC-exo deliver miR-138-5p to target SIRT1 and inhibit the growth and protein expression of human skin fibroblasts, then attenuate HS.<sup>32</sup> However, we further explore whether other genes can also target fibroblasts and the role of MSC-exo in the formation of HS. Thus, our present study investigated the functional changes of hypertrophic scar fibroblast (HSF) under influence of TNFSF13, HSPG2 and MSC-Exo through the HSF model in vitro.

## Materials and Methods

### Ethical Statement

The human subject protocol was approved by the Biomedical Research Ethics Committee of Shandong Provincial Hospital (NSFC: NO.2019-182). All clinical samples were obtained from previously untreated patients with HS at Shandong Provincial Hospital (Shandong, China). Informed consent was obtained from all participants in accordance with the World Medical Association Declaration of Helsinki.

## Human Specimen Collection

The skin tissues of 12 patients with HS were enrolled in this study, and 12 normal skin tissues matched with age and sex were used as controls. The 12 HS tissues were collected from HS patients undergoing scar resection. The 12 normal skin tissues were collected from plastic surgery patients. We obtained tissue from HS patients both at their scar sites and normal skin. All enrolled patients signed written informed consent and the study was approved by the Ethics Committee of our hospital.

## Immunohistochemistry

The HS and normal tissues were fixed with 4% paraformaldehyde, dehydrated with graded ethanol, embedded in paraffin, and then cut into 5  $\mu\text{m}$ -thick sections. After dewaxing with xylene and hydrating with gradient alcohol, sections were heated in microwave oven for antigen repair and then incubated with 3%  $\text{H}_2\text{O}_2$  for 15 min to remove endogenous peroxidase activity. Subsequently, sections were blocked with goat serum for 1 h to prevent non-specific binding. After incubation with primary antibodies (TNFSF13, ab189263, Abcam, Cambridge, UK; Heparan sulfate proteoglycan 2 (HSPG2), ab23418, Abcam, Cambridge, UK; p65, 10745-1-AP, Proteintech, Chicago, USA) overnight at 4 °C, sections were incubated with secondary antibodies (PR30011, Proteintech, Chicago, USA); ab6789, Abcam, Cambridge, UK) for 2 h. The diaminobenzidine was used for color developing. After counterstaining with hematoxylin, sections were dehydrated and vitrified, and finally sealed by resinene. The results were analyzed using ImageJ software.

## Isolation and Culture of Fibroblasts

After the excess subcutaneous fat was removed from skin tissue, the skin tissue was digested with disperse enzyme II (ST2339, Beyotime, Shanghai, China) for 6–8 h to separate the dermis from the epidermis. The dermis was repeatedly cleaned in PBS and cut into small pieces, then incubated in type I collagenase (1 mg/mL, ST2294, Beyotime, Shanghai, China) at 37°C for 6 h. After filtration through a 200-mesh screen, the isolated cells were placed in a DMEM-F12 medium (11320033, Thermo Fisher Scientific, Waltham, MA, USA) containing 10% FBS and 1% penicillin-streptomycin solution (PB180120, Procell, Wuhan, China). All experiments were conducted using third - to fifth-generation cells.

## The Isolation of MSC-Exo

All of these processes have been conducted in our previous study.<sup>32</sup> Here, we use bone marrow mesenchymal stem cells. The cell-conditioned medium was collected from approximately 70% confluent MSC (Cyagen, Guangzhou, China) at a concentration of  $6 \times 10^5$  cells/well grown in 100-mm cell culture dishes with 10mL human MSC basal medium containing FBS depleted of bovine serum extracellular vesicles (JKF1001-100, QIAGEN, Shandong, China) in each dish by 48–36 h. About 1000mL of cell supernatant was collected, and 100mL of cell supernatant was firstly centrifuged at 2000  $\times g$  for 15 min to remove dead cells. Next, the supernatant was centrifuged at 10,000  $\times g$  for 30 min to remove impurities. Then, the supernatant was centrifuged at 120,000  $\times g$  for 70 min using a Ti70 rotor (Optima XPN-100 Ultracentrifuge, Beckman Coulter, Kraemer Boulevard Brea, USA). All centrifugation steps were performed at 4°C. Eventually, exosomes were isolated from the collected medium by differential ultracentrifugation.

## Cell Immunofluorescence

The expression of TNFSF13 and p-p65 in HSF was detected by the immunofluorescence. HSF were seeded on the glass coverslips and incubated in culture dishes for 24 h. Then, HSF were fixed with 4% paraformaldehyde at 25 °C for 15 min. After blocking with goat serum at 25 °C for 1 h, HSF were incubated with primary antibodies (TNFSF13, ab189263, Abcam, Cambridge, UK; p-p65, 3033T, Cell Signaling Technology, Boston, USA) at 4°C overnight, and then incubated with secondary antibody (ab150077, Abcam, Cambridge, UK) at 25 °C for 2h. After counterstaining with DAPI at 25 °C for 5 min, the results were observed under a laser confocal microscope (ZEISS, Oberkochen, Germany).

## Cell Treatment and Transfection

The recombinant human TNFSF13 protein (Sino Biological, Beijing, China) at the dose of 10, 30, and 100 ng/mL was used to treat HSF for 24 h to overexpress TNFSF13. The Nuclear factor- $\kappa\text{B}$  (NF- $\kappa\text{B}$ ) inhibitor, pyrrolidine dithiocarbamate (PDTC, 1 mM, Shanghai yuanye Bio-Technology Co., Ltd), was used to treat HSF for 24 h for inhibiting the NF- $\kappa\text{B}$  signaling pathway.

The siRNAs targeting TNFSF13 (si-TNFSF13-1 and si-TNFSF13-2) and its scrambled control were purchased from RibiBio. si-HSPG2 and its negative control (si-NC) were also from RibiBio. The si-TNFSF13-1/-2 and scrambled siRNA were transfected into HSF by the Lipofectamine 2000 (Thermo Fisher Scientific, Waltham, MA, USA). The sequences were as follows:

si-TNFSF12-1, 5'-GCCAGCCTCATCTCCTTCTT-3';  
si-TNFSF13-2, 5'-GCTCTGCTGACCCAACAAACA-3';  
Scrambled siRNA, 5'-GCCTCCAACCTAACGACTGAA-3';  
si-HSPG2, 5'-GGCATAACGATGGCTTGTCTCT-3';  
si-NC, 5'-GCGTTGCCAAGTCGTTCAAGT-3'.

## CCK-8 Assay

The cell viability of HSF was detected by CCK-8 kit (C0038, Beyotime, Shanghai, China). HSF were seeded into 96-well plate ( $3 \times 10^3$  cells/well) and incubated for 24, 48, and 72 h. The 10  $\mu$ L CCK-8 solution (Elabscience, Wuhan, China) was added into each well. After incubation for 1 h, the absorbance at 450 nm was detected by a microplate reader.

## EdU Staining

The proliferation of HSF was measured by using the EdU cell proliferation kit (C0075S, Beyotime, Shanghai, China). After incubation for 24 h in 24-well plates, HSF were incubated with EdU solution and then fixed with 4% paraformaldehyde for 15 min at 25 °C. After incubation with PBS contained 0.3% Triton X-100 for 15 min, HSF were washed with PBS. Subsequently, HSF were incubated with DAPI for 10 min. The proportion of EdU-positive cells was observed under a laser confocal microscope (ZEISS, Oberkochen, Germany).

## Transwell Migration Assay

The migration of HSF was evaluated by Transwell assay. HSF were seeded in the upper chamber (Millipore, Darmstadt, Germany) with serum-free medium. The lower chamber was added in medium contained 10% FBS. After of 24 h incubation, the cells in upper chamber were removed with cotton ball. The cells on the lower chamber were fixed with 4% paraformaldehyde and stained with 0.5% crystal violet. The migrated cells were calculated under an optical microscope.

## qRT-PCR

The total RNA was extracted from skin tissues and HSF by using the Trizol reagent (R0016, Beyotime, Shanghai, China). The first-strand cDNA was synthesized using HiScript II Reverse Transcriptase (R223-01, Vazyme, Nanjing, China) and then mRNA expression was analyzed by qRT-PCR using ChamQ SYBR qPCR Master Mix (Q311-02, Vazyme, Nanjing, China). The relative mRNA expression of genes was analyzed by  $2^{-\Delta\Delta C_t}$ . The sequences of primers are supplied as Table 1.

## Western Blot

Total protein was isolated from skin tissues and HSF by using the RIPA Lysis Buffer (P0013, Beyotime, Shanghai, China) and the concentration was evaluated by BCA Kit (CW0014S, CWBIO). Protein samples were separated by using 10% SDS-PAGE and then transferred onto the PVDF membranes. After blocking with 5% non-fat milk at 25 °C for 1 h, membranes were incubated with primary antibodies at 4 °C overnight, followed by incubation with secondary antibody (ab205718, Abcam, Cambridge, UK) at 25 °C for 2 h. The protein bands were visualized using the ECL kit (P0018, Beyotime, Shanghai, China) and analyzed using ImageJ software. The primary antibodies including TNFSF13 (ab189263, Abcam, Cambridge, UK), GAPDH (10494-1-AP, Proteintech, Chicago, USA),  $\alpha$ -SMA (14395-1-AP, Proteintech, Chicago, USA), Fibronectin (ab2413, Abcam, Cambridge, UK), Collagen I (72026T, Cell Signaling Technology, Boston, USA), IL-1 $\beta$  (16806-1-AP, Proteintech, Chicago, USA), TNF- $\alpha$  (17590-1-AP, Proteintech, Chicago, USA), TGF- $\beta$ 1 (215715, Abcam, Cambridge, UK), HSPG2 (19675-1-AP, Proteintech, Chicago, USA), p65 (10745-1-AP, Proteintech, Chicago, USA), p-p65 (3033T, Cell Signaling Technology, Boston, USA).

## The Identification of MSC-Exo

All of these processes have been conducted in our previous study.<sup>32</sup> About 10  $\mu$ L of isolated exosomes were resuspended in 200  $\mu$ L PBS, the morphology of isolated exosomes was immediately visualized by transmission electron microscope (TEM;



**Table 1** Primary Sequences for PCR

Genes	Primary Sequences
TNFSF13	CAGAGCCTCAGGAGAGAGGT
	GCAGGACAGAGTGCTGCT
$\alpha$ -SMA	ACTGCCTTGGTGTGTGACAA
	CACCATCACCCCCTGATGTC
FNI	CTGGGTCTCCTCCCAGAGAA
	GGGGAAGCTCGTCTGTCTTT
COL1A1	CCCCGAGGCTCTGAAGGT
	GCAATACCAGGAGCACCATTTG
IL-1 $\beta$	TTCGAGGCACAAGGCACAA
	TGGCTGCTTCAGACACTTGAG
TNF- $\alpha$	CCCCAGGGACCTCTCTCTAA
	GCTTGAGGGTTTGCTACAACA
TGF- $\beta$ 1	GGAAATTGAGGGCTTTCGCC
	CCGGTAGTGAACCCGTTGAT
HSPG2	CCTGACGGCCACTTCTACC
	GCATTGTCACATTCACACCCTT
$\beta$ -actin	ACAGAGCCTCGCCTTTGCC
	GATATCATCATCCATGGTGAGCTGG

HT7800, Hitachi), and the distribution of size was analyzed by nanoparticle tracking analysis (NTA; Particle Metrix, ZetaView PMX110). Meanwhile, immunoblotting was performed to detect the expression of known exosomal markers CD9, CD81, and TSG101. Exosome diluted in culture medium was passed through a 0.22- $\mu$ m filter to keep sterilized before the experiment started. The extra exosome precipitation was redissolved with PBS and stored at  $-80^{\circ}\text{C}$  for standby.

## Bioinformatic Analysis

The interaction relationship between TNFSF13 and HSPG2 was plotted by the genemania. The downstream genes of TNFSF13 were enriched by String to analyze the downstream signaling pathways regulated by TNFSF13.

## Statistical Analysis

The data in this study was presented as mean  $\pm$  SD and analyzed by GraphPad Prism 7.0. The difference between two groups was analyzed by Student's *t*-test. The differences among multiple groups were analyzed by one way-ANOVA followed by post hoc Bonferroni's test.  $P < 0.05$  was considered as significant.

## Results

### The Expression of TNFSF13 in Skin Tissues of Patients with HS

The expression of TNFSF13 in tissues of normal skin (NS) and HS was measured by IHC, qRT-PCR, and Western blot. The IHC results showed that TNFSF13 expression in HS skin tissues was significantly higher than NS and was mainly expressed in the dermis (Figure 1A). The data of Figure 1B and C also showed that TNFSF13 mRNA and protein

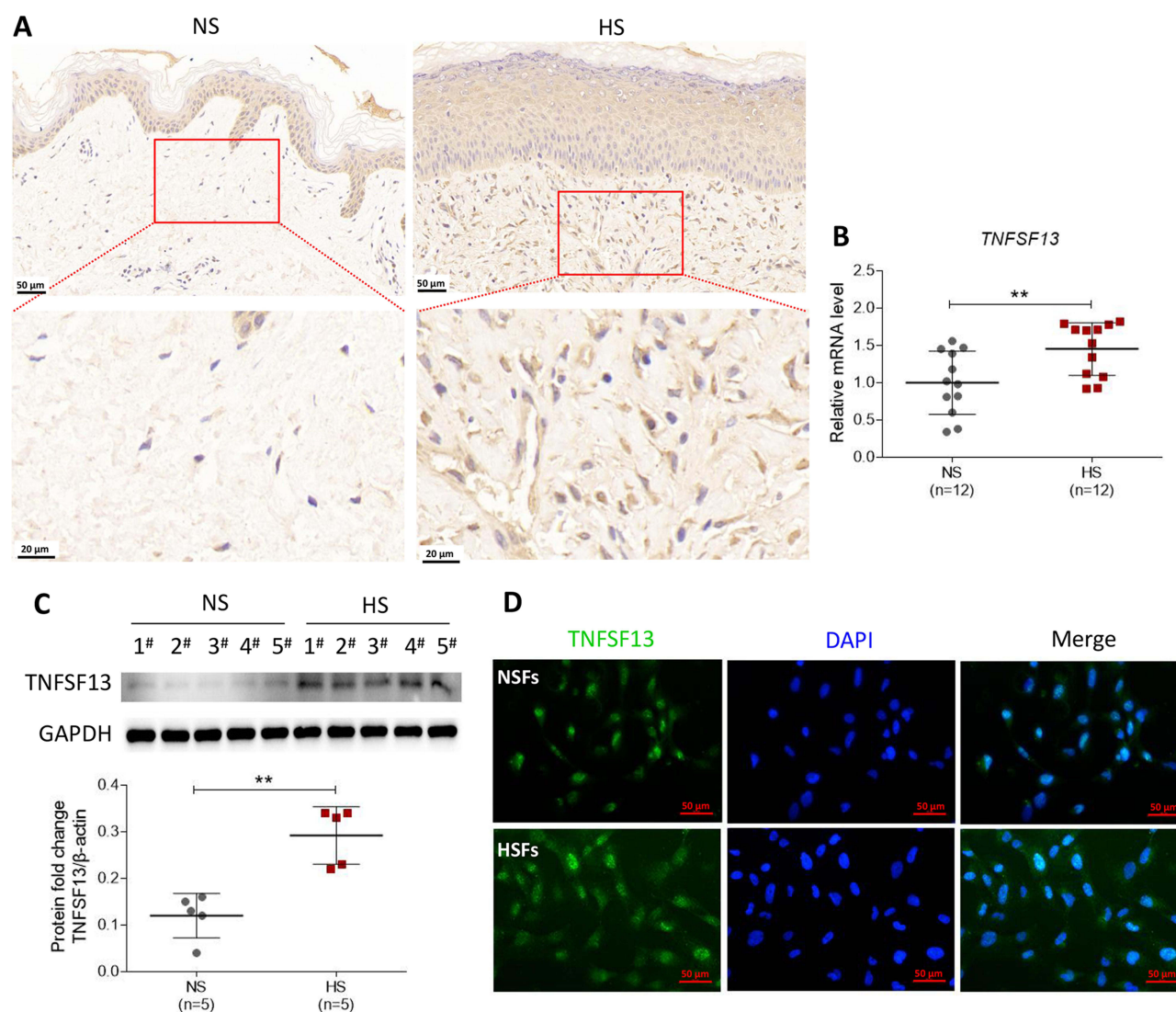


**Figure 1** The expression of *TNFSF13* in skin tissues of patients with HS. **(A)** The *TNFSF13* expression in normal and HS skin tissues was detected by immunohistochemical staining. **(B)** The *TNFSF13* expression in normal and HS skin tissues was detected by qRT-PCR. **(C)** The *TNFSF13* expression in normal and HS skin tissues was detected by Western blot. **(D)** The *TNFSF13* expression in NSF and HSF was detected by cell immunofluorescence. \*\* $P < 0.01$ .

expression were markedly increased in HS skin tissues compared with NS skin tissues. Subsequently, the HSF and NSF were isolated from NS and HS skin tissues, respectively. Cell immunofluorescence was performed to evaluate intracellular *TNFSF13* expression. *TNFSF13* expression was relatively higher in HSF than in NSF, and *TNFSF13* was mainly expressed in cytoplasm (Figure 1D).

## The Function of *TNFSF13* on the Proliferation and Migration of HSF

Different doses of recombinant *TNFSF13* proteins and *TNFSF13* siRNAs were used to treat HSF to detect the role of *TNFSF13* on HSF. The CCK-8 data showed that recombinant *TNFSF13* protein markedly increased the cell viability of HSF, while *TNFSF13* siRNAs markedly decreased the viability of HSF (Figure 2A and B). EdU staining showed that the EdU-positive cells were markedly increased in HSF after recombinant *TNFSF13* protein treatment (Figure 2C). Oppositely, *TNFSF13* siRNAs remarkably reduced the number of EdU-positive cells (Figure 2D). Besides, the migrated cells were significantly increased by recombinant *TNFSF13* protein treatment, while markedly decreased by *TNFSF13* siRNAs (Figure 2E and F).

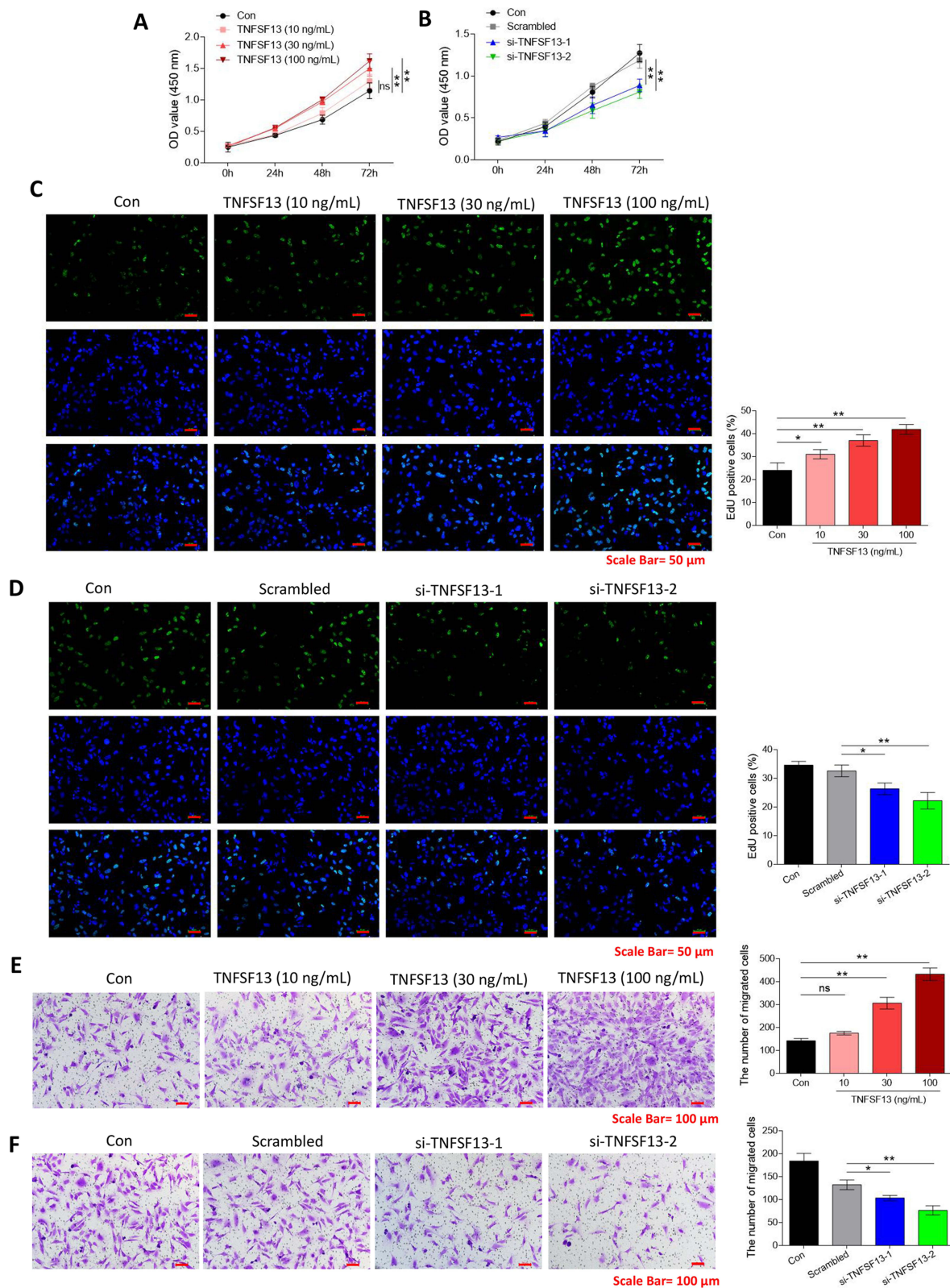


**Figure 2** The function of TNFSF13 on the proliferation and migration of HSF. The cell viability of HSF (A) after treatment with different doses of TNFSF13 and (B) transfection with TNFSF13 siRNAs was detected by CCK-8 assay. The proliferation of HSF (C) after treatment with different doses of TNFSF13 and (D) transfection with TNFSF13 siRNAs was detected by EdU staining. The cell migration of HSF (E) after treatment with different doses of TNFSF13 and (F) transfection with TNFSF13 siRNAs was detected by Transwell assay. \* $P < 0.05$ , \*\* $P < 0.01$ .



## The Function of TNFSF13 on the Fibrosis and Inflammation of HSF

Then, the expression of fibrosis-associated genes and proteins was evaluated by qRT-PCR and Western blot. The data showed that recombinant TNFSF13 protein treatment dramatically increased the expression of  $\alpha$ -SMA, FN1, and COL1A1 in HSF (Figure 3A and B). On the contrary, TNFSF13 siRNAs significantly reduced the expression of  $\alpha$ -SMA, FN1, and COL1A1 in HSF (Figure 3C and D). The levels of the expression of inflammation cytokines IL-1 $\beta$ , TNF- $\alpha$ , and TGF- $\beta$ 1 in HSF were markedly raised by recombinant TNFSF13 protein, while decreased by TNFSF13 siRNAs (Figure 3E–H).

## Binding of TNFSF13 and HSPG2 in HSF Activates NF- $\kappa$ B Signaling Pathway

TNFSF13 and HSPG2 have been widely reported as ligand–receptor relationships. The interaction between TNFSF13 and HSPG2 was plotted by genemania (Figure 4A). Subsequently, the downstream signaling pathways of TNFSF13 on HSF were analyzed by using String. The analysis showed that NF- $\kappa$ B signaling pathway was the downstream signaling pathway of TNFSF13 in HSF (Figure 4B). The addition of TNFSF13 significantly promoted the phosphorylation of p65,

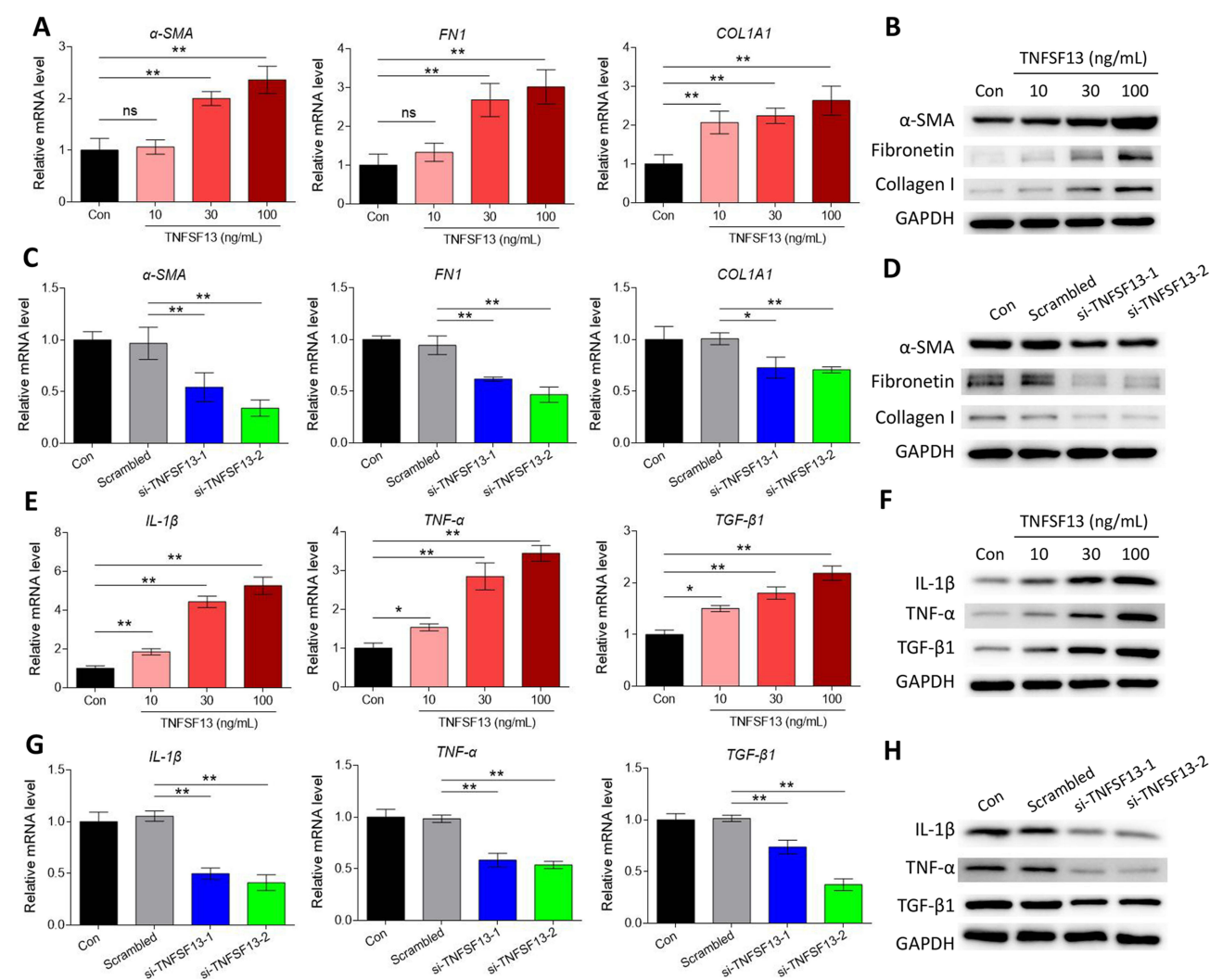


**Figure 3** The function of TNFSF13 on the fibrosis and inflammation of HSF. The expression of fibrosis-associated genes  $\alpha$ -SMA, FN1, and COL1A1 in HSF (A) after treatment with different doses of TNFSF13 and (C) transfection with TNFSF13 siRNAs were detected by qRT-PCR. The expression of fibrosis-associated proteins  $\alpha$ -SMA, Fibronectin, and Collagen I in HSF (B) after treatment with different doses of TNFSF13 and (D) transfection with TNFSF13 siRNAs were detected by Western blot. The expression of inflammation cytokines IL-1 $\beta$ , TNF- $\alpha$ , and TGF- $\beta$ 1 in HSF (E) after treatment with different doses of TNFSF13 and (G) transfection with TNFSF13 siRNAs were detected by qRT-PCR. The expression of inflammation cytokines IL-1 $\beta$ , TNF- $\alpha$ , and TGF- $\beta$ 1 in HSF (F) after treatment with different doses of TNFSF13 and (H) transfection with TNFSF13 siRNAs were detected by Western blot. \*P<0.05, \*\*P<0.01.

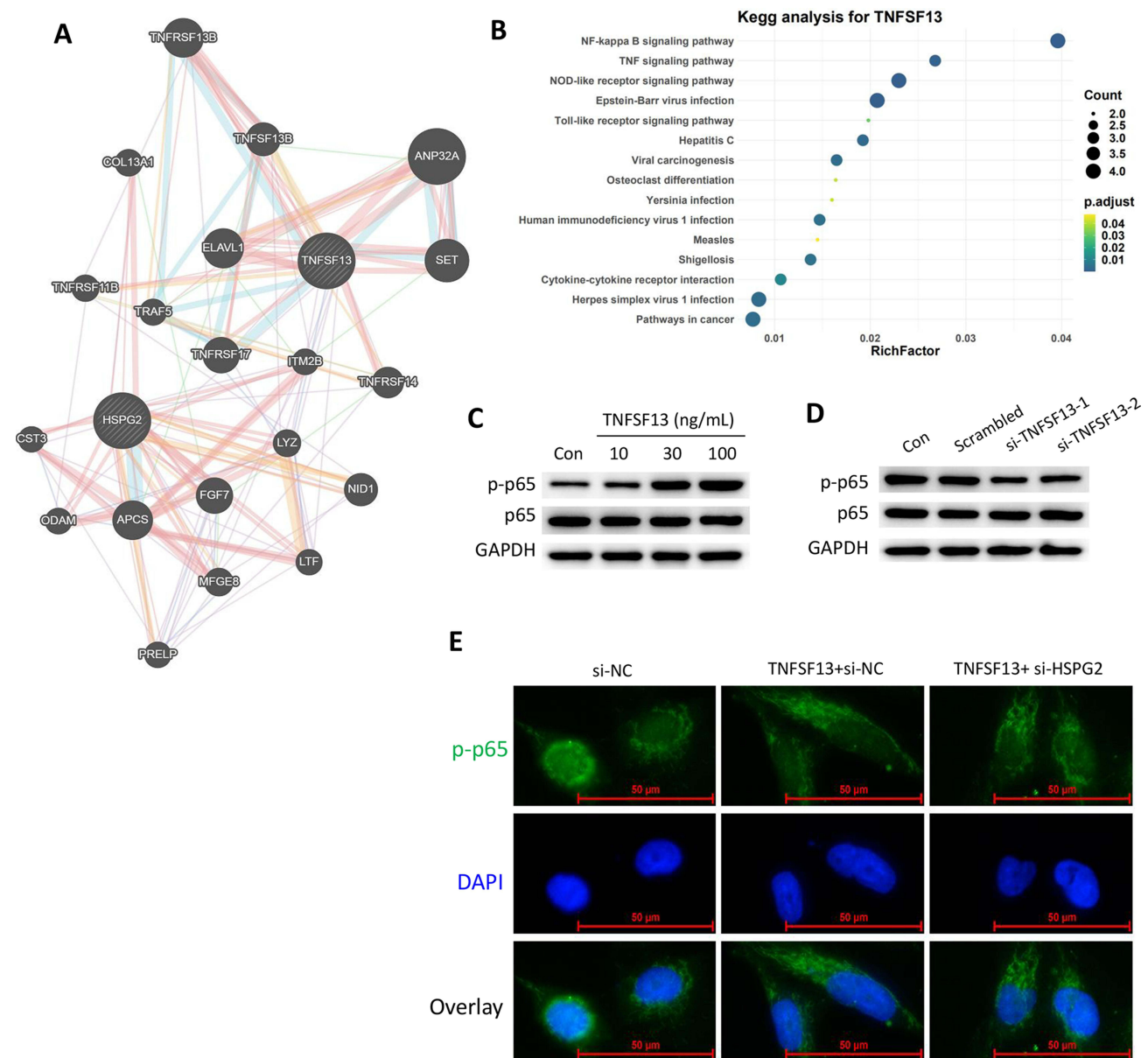


**Figure 4** Binding of TNFSF13 and HSPG2 in HSF activates NF- $\kappa$ B signaling pathway. **(A)** The interaction between TNFSF13 and HSPG2 was analyzed by genemania. **(B)** The interaction between TNFSF13 and HSPG2 was confirmed by CO-IP assay. The downstream signaling pathways of TNFSF13 were analyzed by String. **(C/D)** The protein expression and phosphorylation of p65 after treatment with different doses of TNFSF13 and transfection with TNFSF13 siRNAs was detected by Western blot. **(E)** The nuclear translocation of p-p65 was detected by cell immunofluorescence.

while TNFSF13 siRNAs inhibited the phosphorylation of p65 (Figure 4C and D). Additionally, the immunofluorescence showed a large number of p-p65 nuclear translocations in recombinant TNFSF13 protein-treated HSF (Figure 4E). However, silencing of HSPG2 markedly inhibited the nuclear translocation of p-p65.

## The Expression of HSPG2 and p65 in Skin Tissues of Patients with HS

The expression of HSPG2 and p65 in skin tissues of NS and HS was then evaluated by IHC. The expression of HSPG2 and p65 in HS tissues was markedly increased compared with NS skin tissues (Figure 5A). *HSPG2* mRNA expression in NS skin tissues was dramatically increased in comparison with HS skin tissues (Figure 5B). Additionally, the protein expression of HSPG2 and p-p65/p65 in skin tissues was detected by Western blot. The levels of HSPG2 and p-p65/p65 were remarkably higher in HS tissues than that in NS skin tissues (Figure 5C and D).



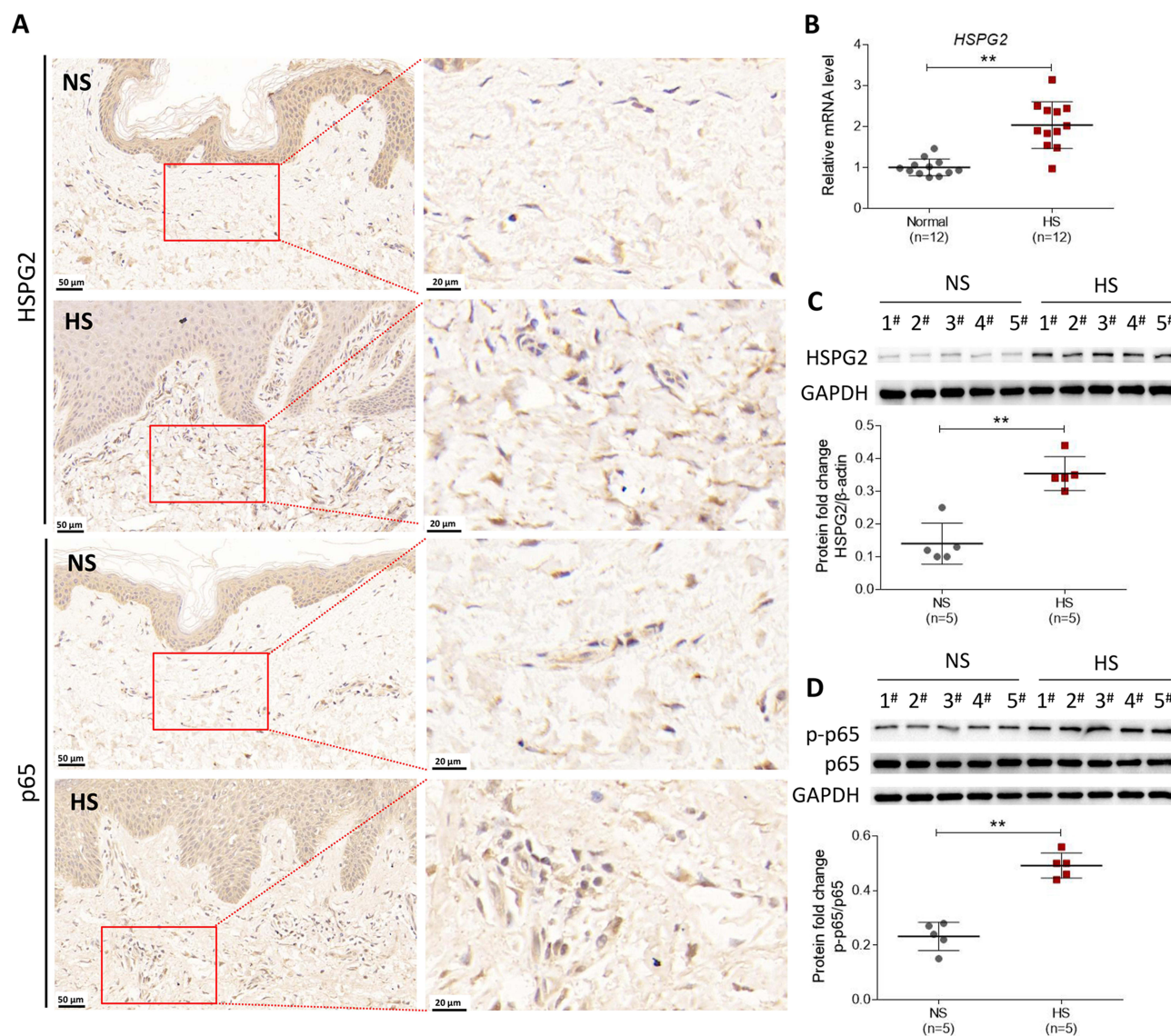


**Figure 5** The expression of HSPG2 and p65 in skin tissues of patients with HS. **(A)** The expression of HSPG2 and p65 in skin tissues of NS and HS was detected by immunohistochemical staining. **(B)** The expression of HSPG2 in skin tissues of NS and HS was detected by qRT-PCR. The protein expression of **(C)** HSPG2 and **(D)** p65, and p-p65 was detected by Western blot. \*\* $P < 0.01$ .

## Inhibition of HSPG2 and NF- $\kappa$ B Reverses the Effects of TNFSF13 on HSF Proliferation and Migration

To verify the regulatory relationship between HSPG2, NF- $\kappa$ B and TNFSF13 in HS, HSPG2 was silenced by siRNA transfection and NF- $\kappa$ B signaling was inhibited using PDTC in HSF. TNFSF13 treatment remarkably increased the cell viability of HSF. However, the effect of TNFSF13 on cell viability of HSF was obviously eliminated by both si-HSPG2 and PDTC (Figure 6A and B). The EdU results showed that TNFSF13 treatment significantly promoted proliferation of HSF. However, si-HSPG2 and PDTC dramatically eliminated the promoting effect of TNFSF13 on proliferation of HSF (Figure 6C and D). The Transwell assay suggested that TNFSF13 treatment markedly enhanced the migration ability of HSF. Compared with TNFSF13 group, the migration in si-HSPG2 and PDTC treated groups was significantly decreased (Figure 6E and F).

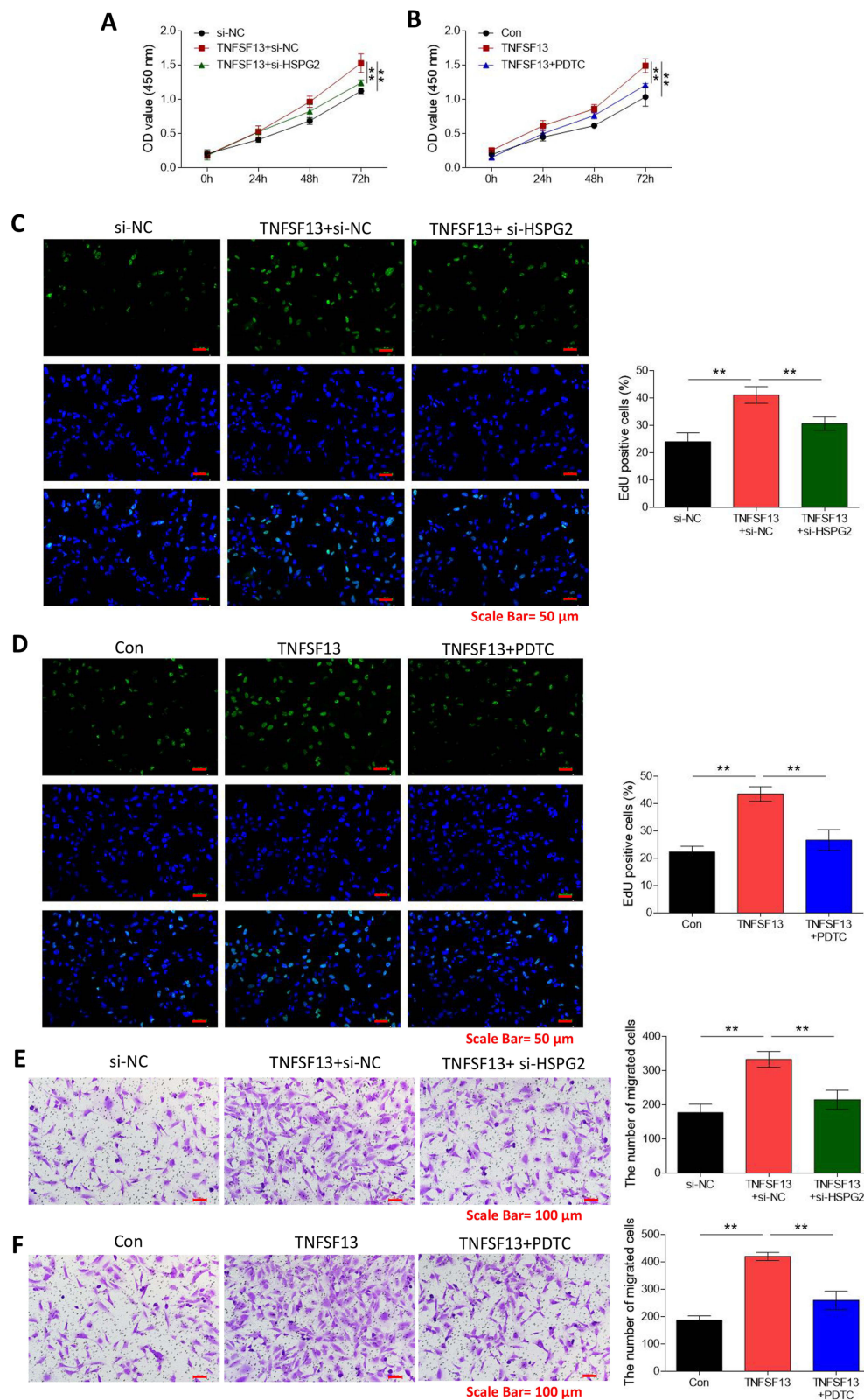


**Figure 6** Inhibition of HSPG2 and NF- $\kappa$ B reverses the effects of TNFSF13 on HSF proliferation and migration. The cell viability of HSF after (A) transfection with si-HSPG2 or (B) co-treatment with TNFSF13 and PDTC was detected by CCK-8 assay. The proliferation of HSF after (C) transfection with si-HSPG2 or (D) co-treatment with TNFSF13 and PDTC was detected by EdU staining. The cell migration of HSF after (E) transfection with si-HSPG2 or (F) co-treatment with TNFSF13 and PDTC was detected by Transwell assay. \*\* $P < 0.01$ .

# Inhibition of HSPG2 and NF- $\kappa$ B Reverses the Effects of TNFSF13 on HSF Fibrosis and Inflammation

The data showed that TNFSF13 treatment significantly increased the mRNA levels of  $\alpha$ -SMA, *FN1*, and *COL1A1* in HSF (Figure 7A and C). The Western blot data showed that TNFSF13 treatment markedly raised the protein levels of  $\alpha$ -SMA, Fibronectin, and Collagen I of HSF (Figure 7B and D). Significantly, the promoting effect of TNFSF13 on fibrosis-associated genes was eliminated by si-HSPG2 and PDTC. The mRNA levels of  $\alpha$ -SMA, *FN1*, and *COL1A1* and protein levels of  $\alpha$ -SMA, Fibronectin, and Collagen I in si-HSPG2 and PDTC treated groups were remarkably decreased in comparison with TNFSF13 group (Figure 7A–D). The data in Figure 7E–H showed that TNFSF13 treatment markedly increased the levels of inflammation cytokines IL-1 $\beta$ , TNF- $\alpha$ , and TGF- $\beta$ 1 in HSF. Obviously, both si-HSPG2 and PDTC suppressed the promoted effect of TNFSF13 on inflammation cytokines. The levels of inflammation cytokines in si-HSPG2 and PDTC treated groups were dramatically decreased compared with TNFSF13 group (Figure 7E–H).

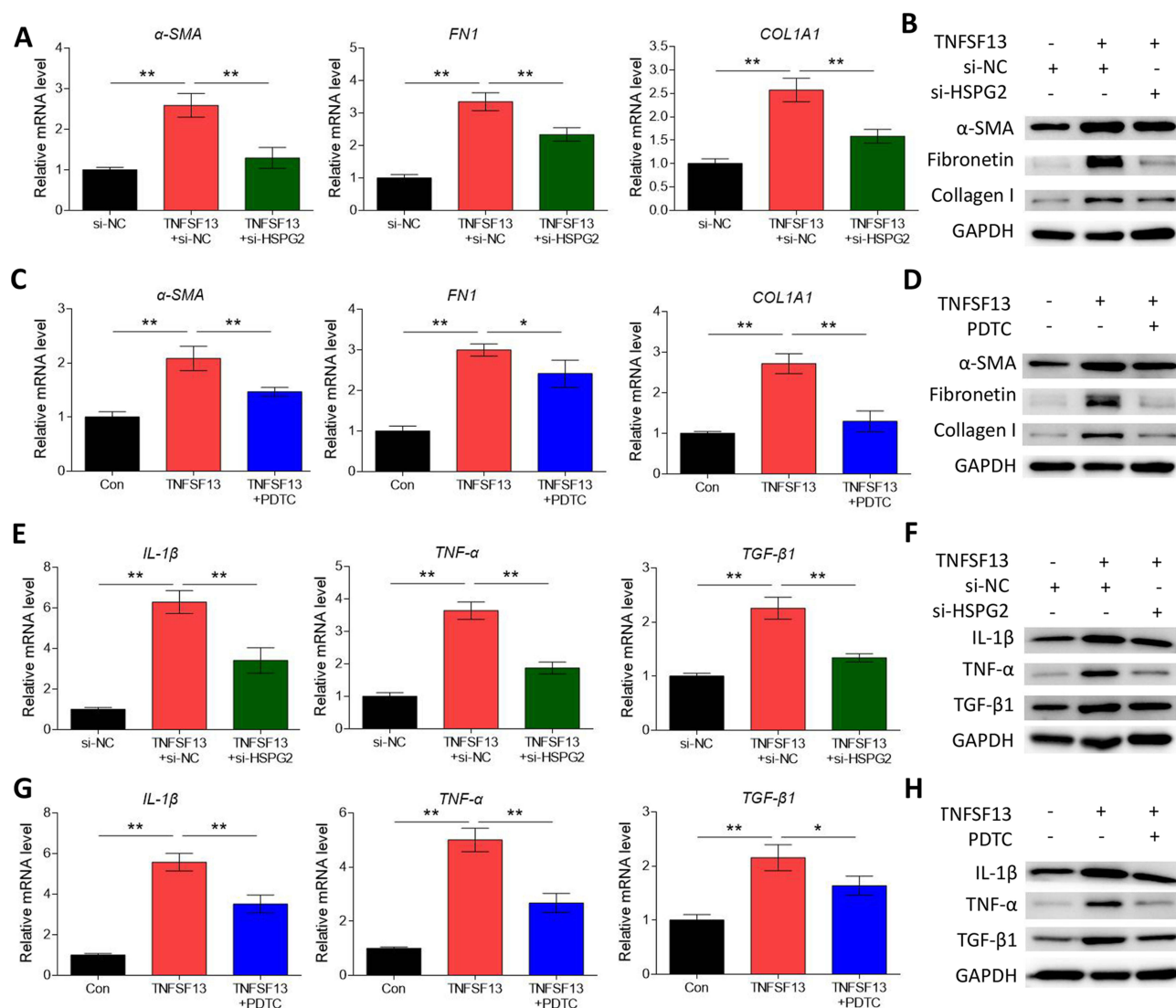


**Figure 7** Inhibition of HSPG2 and NF- $\kappa$ B reverses the effects of TNFSF13 on HSF fibrosis and inflammation. The expression of fibrosis-associated genes  $\alpha$ -SMA, *FN1*, and *COL1A1* in HSF after (A) transfection with si-HSPG2 or (C) co-treatment with TNFSF13 and PDTC were detected by qRT-PCR. The expression of fibrosis-associated proteins  $\alpha$ -SMA, Fibronectin, and Collagen I in HSF after (B) transfection with si-HSPG2 or (D) co-treatment with TNFSF13 and PDTC were detected by Western blot. The expression of inflammation cytokines *IL-1 $\beta$* , *TNF- $\alpha$* , and *TGF- $\beta$ 1* in HSF after (E) transfection with si-HSPG2 or (G) co-treatment with TNFSF13 and PDTC were detected by qRT-PCR. The expression of inflammation cytokines *IL-1 $\beta$* , *TNF- $\alpha$* , and *TGF- $\beta$ 1* in HSF after (F) transfection with si-HSPG2 or (H) co-treatment with TNFSF13 and PDTC were detected by Western blot. \* $P$ <0.05, \*\* $P$ <0.01.



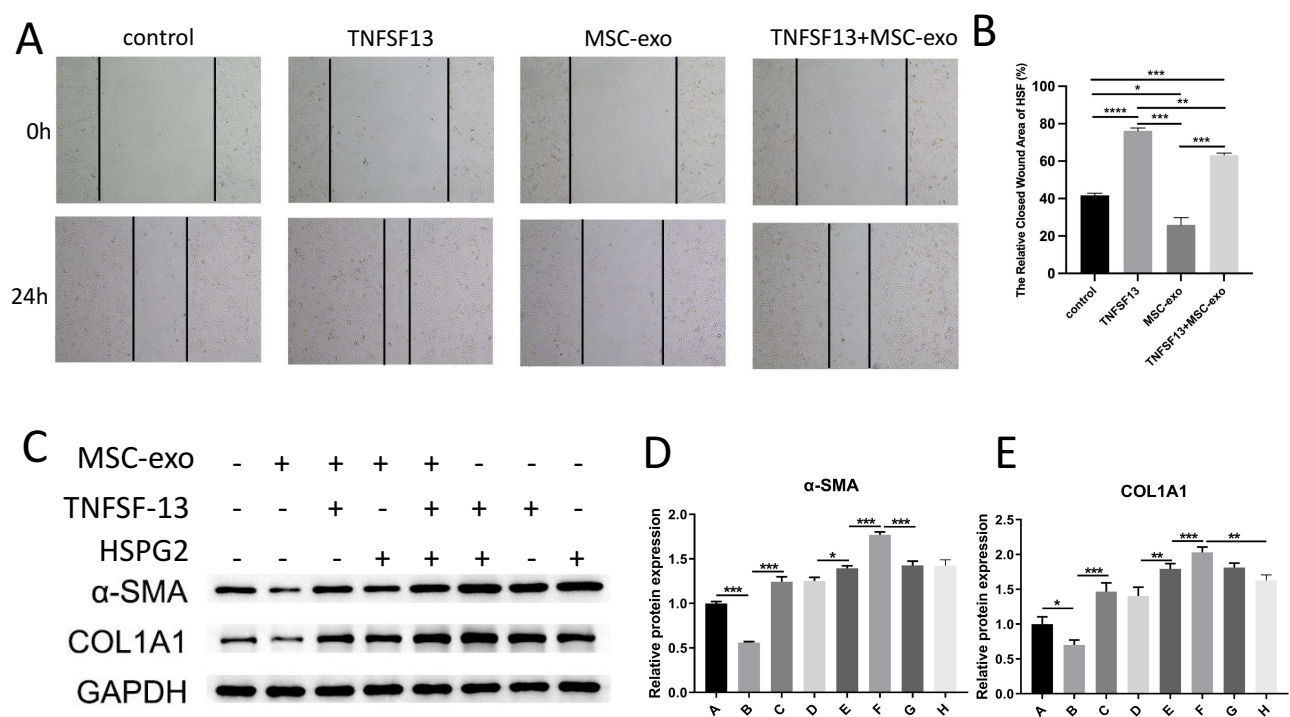


**Figure 8** Effect of MSC-exo on the proliferation and migration of HSF. (A and B) Scratch analysis of the migration of HSF transfected with control, TNFSF13, MSC-exo and TNFSF13+MSC-exo at 0-, 24h, graph showed the relative closed wound area of HSF. (C–E) Western blot analysis of  $\alpha$ -SMA and COL1A1 in HSF stimulated with PBS, MSC-exo, MSC-exo+TNFSF13, MSC-exo+HSPG2, MSC-exo+TNFSF13+HSPG2, TNFSF13+HSPG2, TNFSF13, HSPG2 for 48h, graph showed the relative band density to GAPDH. Every experiment was repeated at least three times, and the data was shown as mean  $\pm$  SEM (\* $P$ <0.05, \*\* $P$ <0.01, \*\*\* $P$ <0.001, \*\*\*\* $P$ <0.0001).

## MSC-Exo Inhibits the Proliferation and Migration of HSF by Inhibiting TNFSF13 and HSPG2

To explore whether MSC-exo could influence the biological behaviors of HSF, we conducted scratch and Western blot to measure the proliferation and migration of HSF. Scratch assay showed that TNFSF13 significantly promoted the migration of HSF, whereas MSC-exo showed an obvious effect on inhibiting the migration of HSF. TNFSF13+ MSC-exo together partly promoted the migration of HSF compared with MSC-exo only, but partly inhibited the migration of HSF compared with TNFSF13 only (Figure 8A and B). To test whether MSC-exo could inhibit collagen deposition and the expression of profibrotic protein of HSF, Western blot analysis was performed to evaluate the expression levels of  $\alpha$ -SMA and COL1A1 in different groups of HSF. The data demonstrated that MSC-exo significantly inhibited the expression levels of  $\alpha$ -SMA and COL1A1 (Figure 8C–E).

## Discussion

HS is a common complication during wound healing.<sup>33</sup> In the process of wound healing, fibroblasts were transformed into myofibroblasts with strong  $\alpha$ -SMA expression and abnormal proliferation, with vigorous collagen secretion and disordered arrangement, leading to the formation of HS.<sup>34</sup> Moreover, immune cells play an important role in the process of wound healing, which are recruited to accumulate in the injured area under the action of chemokines, and secrete a variety of inflammatory cytokines, inducing more immune cells to participate in the inflammatory reaction at the injured area. In addition, the cytokines secreted by these immune cells can promote the proliferation and migration of fibroblasts and produce new ECM.<sup>35</sup> Although the immune cells and mechanisms involved in wound repair have been extensively studied, the principles of regulating the biological activity of fibroblasts are only partially understood.<sup>36</sup> The present study demonstrated that TNFSF13 interacting with HSPG2 to activate NF- $\kappa$ B pathway could promote the proliferation, migration, fibrosis, and inflammation of HSF, whereas MSC-exo could inhibit the effect of TNFSF13 on fibroblasts.

TNFSF13, which has been identified as proinflammatory mediator, participates in various innate and adaptive immunity processes.<sup>37</sup> It has been reported TNFSF13 can regulate cell proliferation, cell death, development, survival, immunity, and various diseases, play broad biological roles in immunity system. A previous study demonstrated that expression of TNFSF13 was increased at 14 days after spinal cord injury, leading to form the fibrotic scar.<sup>25</sup> In another study, TNFSF13 is highly expressed in tumor cells and fibroblasts in a cohort of patients with non-small cell lung cancer (NSCLC) were analyzed by quantitative real-time polymerase-chain reaction.<sup>38</sup> Our group has pioneered work implicating the TNFSF13 in HSF. We believe targeting this superfamily remains key to improve efficacy and selectivity of currently available therapies for HS. In our study, TNFSF13 was up-regulated in HS skin tissues and HSF (Figure 1). The proliferation and migration of HSF were markedly increased by addition of recombinant TNFSF13 protein while suppressed by TNFSF13 siRNAs (Figure 2). Furthermore, recombinant TNFSF13 protein increased the expression of fibrosis associated proteins  $\alpha$ -SMA, fibronectin and fibrous collagen protein collagen I in HSF. TNFSF13 siRNAs markedly inhibited the expression of these genes and proteins. Additionally, the levels of inflammation cytokines IL-1 $\beta$ , TNF- $\alpha$ , and TGF- $\beta$ 1 were also raised by recombinant TNFSF13 protein and reduced by TNFSF13 siRNAs (Figure 3). These findings suggested that TNFSF13 promoted the proliferation and migration of HSF and the accumulation of ECM, thus promoting HS development.

HSPG receptor is a kind of biological macromolecule widely existing in cell membrane and cell matrix, which is mainly composed of a core protein linked to heparin sulfate sugar chain through Covalent bond. HSPG plays an important role in a series of processes such as cell proliferation, differentiation, invasion, and metastasis. In Zhou's study, wound healing was delayed, granulation tissue formation was reduced in HSPG knockdown mice.<sup>39</sup> Moreover, Chen et al investigated that HSPG was overexpressed in the fibroblasts from the scar area of patients with chronic fibrotic disorder diffuse scleroderma (diffuse systemic sclerosis), and the adhesion and contraction ability of fibroblasts was significantly weakened by blocking its cellular HSPG activity. Ultimately, it was found that HSPG reduce scar formation in chronic fibrosis.<sup>40</sup> Based on this, we speculate that TNFSF13 may regulate HSPG signal pathway mediate the formation of HS. In this study, we plotted the interaction between TNFSF13 and HSPG2 using genemania (Figure 4A). Moreover, HSPG2 was highly expressed in HS skin tissue and HSF (Figure 5). The results showed that the proliferation and migration of HSF promoted by TNFSF13 recombinant protein, as well as the elevated levels of fibrosis-related proteins and inflammatory cytokines were significantly inhibited by silencing of HSPG2 (Figure 6). These data showed that TNFSF13 interacted with HSPG2 to regulate HSF proliferation, migration, fibrosis, and inflammation.

NF- $\kappa$ B is a family of dimer transcription factors critical for coordinating inflammation, immunity, cell proliferation, and survival.<sup>41,42</sup> TNFSF13 has been shown to be involved in a variety of physiological developments by mediating the NF- $\kappa$ B signaling pathway.<sup>43,44</sup> TNFSF13 induced cisplatin resistance in gastric cancer cells by activating the NF- $\kappa$ B pathway. TNFSF13 is involved in mitochondrial and endoplasmic reticulum stress-induced memory plasma cell death through NF- $\kappa$ B signaling.<sup>45</sup> Pyrrolidine dithiocarbamate (PDTC) is a type of NF- $\kappa$ B signal pathway inhibitor, which can block the degradation of I $\kappa$ B to inhibit NF- $\kappa$ B signal pathway activation, while inhibiting NF- $\kappa$ B Transferring into the nucleus, thereby blocking the action of NF- $\kappa$ B signal pathway.<sup>46</sup> The current study revealed that the phosphorylation of p65 was remarkably increased in HS skin tissues and HSF (Figure 5A). After treatment with NF- $\kappa$ B inhibitor PDTC, the proliferation and migration were markedly inhibited, the expression of fibrosis-related genes  $\alpha$ -SMA, fibronectin, collagen I and inflammation cytokines were also reduced (Figure 7). These results suggested that the regulatory effect of TNFSF13 on HSF was achieved by the NF- $\kappa$ B signaling pathway.

MSC, a subgroup of heterogeneous non-hematopoietic fibroblast-like cells, have high differentiation potential and immune regulatory function. And they are mainly obtained from various tissues including bone marrow, umbilical cord, amniotic fluid, dental pulp, fat tissues, menstrual blood.<sup>47</sup> EXOs, with the diameter of 30 to 150 nm, are nanoscale vesicles secreted by cells through exocytosis, especially MSC, which contain proteins, lipids, nucleic acids and other biological information.<sup>48</sup> Lots of studies showed that exosomes can be used as nanocarriers to transport functional cargos (such as growth factor, cytokine, miRNA, etc.) to regulate the activity of recipient cells, and to deliver active factors or small molecules to recipient cells.<sup>49</sup> As an alternative in more bio-stable material, one of the most important applications for exosomes is drug delivery systems. Rezakhani et al reported that crab haemolymph exosomes have antioxidant properties, carrying anticancer drugs and other drugs, which can inhibit the proliferation of mouse breast cancer cells.<sup>50</sup>



Rashidi et al investigated that Milk-derived exosomes delivering miRNA-320, 375, and Let-7 can be used to treat necrotizing enterocolitis by reducing the expression of interleukin 6 and tumor necrosis factor- $\alpha$ .<sup>51</sup> MSC-exo is also applied in wound healing and tissue repair as well as scar attenuation. In a previous study showed that MSC-exo could promote neovascularization via the PI3K/AKT pathway and enhance skin wound recovery in the diabetic skin wound animal model.<sup>52</sup> We investigated MSC-exo could inhibit the proliferation and migration of HSF by downregulating SIRT1 via miR-138-5p to alleviate HS.<sup>32</sup> In our present study, MSC-exo could suppress the migration and protein expression of HSF by inhibiting TNFSF13 and HSPG2 (Figure 8).

Here, we described a process by which MSC-exo regulates migration of HSF and the expression levels of downstream inflammatory and profibrotic proteins in HSF, including  $\alpha$ -SMA and COL1A1, by inhibiting TNFSF13 and HSPG2.

## Conclusion

This study confirmed that TNFSF13 is up-regulated in HS tissue and HSF. TNFSF13 regulated the proliferation, migration, fibrosis and inflammation of HSF by interacting with HSPG2 to activate NF- $\kappa$ B pathway. Whereas MSC-exo reduced the expression levels of  $\alpha$ -SMA and COL1A1 and inhibited the proliferation, migration, fibrosis and inflammatory reaction of HSF. These results suggest that MSC-exo alleviates HS by inhibiting the fibroblasts via TNFSF-13/HSPG2 signaling pathway.

## Acknowledgments

Thanks to the funding of the National Natural Science Foundation of China (81901968), the Provincial Natural Science Foundation of Shandong province (ZR2019BH051) and the Postdoctoral Science Foundation of China (2018M642667).

## Funding

This study was financially supported by the National Natural Science Foundation of China (81901968), the Provincial Natural Science Foundation of Shandong province (ZR2019BH051) and the Postdoctoral Science Foundation of China (2018M642667).

## Disclosure

The authors report no conflicts of interest in this work.

## References

- Diegidio P, Hermiz S, Hibbard J, Kosorok M, Hultman CS. Hypertrophic burn scar research: from quantitative assessment to designing clinical sequential multiple assignment randomized trials. *Clin Plast Surg*. 2017;44(4):917–924. doi:10.1016/j.cps.2017.05.024
- Matiasek J, Kienzl P, Unger LW, Grill C, Koller R, Turk BR. An intra-individual surgical wound comparison shows that octenidine-based hydrogel wound dressing ameliorates scar appearance following abdominoplasty. *Int Wound J*. 2018;15(6):914–920. doi:10.1111/iwj.12944
- Weng W, He S, Song H, et al. Aligned carbon nanotubes reduce hypertrophic scar via regulating cell behavior. *ACS nano*. 2018;12(8):7601–7612. doi:10.1021/acsnano.7b07439
- Qian H, Shan Y, Gong R, et al. Fibroblasts in scar formation: biology and clinical translation. *Oxid Med Cell Longev*. 2022;2022:4586569. doi:10.1155/2022/4586569
- Chun Q, ZhiYong W, Fei S, XiQiao W. Dynamic biological changes in fibroblasts during hypertrophic scar formation and regression. *Int Wound J*. 2016;13(2):257–262. doi:10.1111/iwj.12283
- Finnerty CC, Jeschke MG, Branski LK, Barret JP, Dziewulski P, Herndon DN. Hypertrophic scarring: the greatest unmet challenge after burn injury. *Lancet*. 2016;388(10052):1427–1436. doi:10.1016/S0140-6736(16)31406-4
- Song J, Li X, Li J. Emerging evidence for the roles of peptide in hypertrophic scar. *Life Sci*. 2020;241:117174. doi:10.1016/j.lfs.2019.117174
- Zhang J, Li Y, Liu J, et al. Adiponectin ameliorates hypertrophic scar by inhibiting Yes-associated protein transcription through SIRT1-mediated deacetylation of C/EBP $\beta$  and histone H3. *iScience*. 2022;25(10):105236. doi:10.1016/j.isci.2022.105236
- Lee Peng G, Kerolus JL. Management of surgical scars. *Facial Plast Surg Clin North Am*. 2019;27(4):513–517. doi:10.1016/j.fsc.2019.07.013
- Hietanen KE, Järvinen TA, Huhtala H, Tolonen TT, Kuokkanen HO, Kaartinen IS. Treatment of keloid scars with intralesional triamcinolone and 5-fluorouracil injections - a randomized controlled trial. *J Plast Reconstr Aesthet Surg*. 2019;72(1):4–11. doi:10.1016/j.bjps.2018.05.052
- Chen Z, Chen Z, Pang R, et al. The effect of botulinum toxin injection dose on the appearance of surgical scar. *Sci Rep*. 2021;11(1):13670. doi:10.1038/s41598-021-93203-x
- Ogawa R, Dohi T, Tosa M, Aoki M, Akaishi S. The latest strategy for keloid and hypertrophic scar prevention and treatment: the Nippon Medical School (NMS) Protocol. *J Nippon Med Schl*. 2021;88(1):2–9. doi:10.1272/jnms.JNMS.2021\_88-106

13. Yao Y, Jiang Y, Song J, et al. Exosomes as potential functional nanomaterials for Tissue Engineering. *Adv Healthcare Mater.* 2023;12(16): e2201989. doi:10.1002/adhm.202201989
14. Casado JG, Blázquez R, Vela FJ, Álvarez V, Tarazona R, Sánchez-Margallo FM. Mesenchymal stem cell-derived exosomes: immunomodulatory evaluation in an antigen-induced synovitis porcine model. *Front Vet Sci.* 2017;4:39. doi:10.3389/fvets.2017.00039
15. Khazaei F, Rezakhani L, Alizadeh M, Mahdavian E, Khazaei M. Exosomes and exosome-loaded scaffolds: characterization and application in modern regenerative medicine. *Tissue Cell.* 2023;80:102007. doi:10.1016/j.tice.2022.102007
16. Tenchov R, Sasso JM, Wang X, Liaw WS, Chen CA, Zhou QA. Exosomes—Nature's Lipid Nanoparticles, a rising star in drug delivery and diagnostics. *ACS nano.* 2022;16(11):17802–17846. doi:10.1021/acsnano.2c08774
17. Rahmati S, Khazaei M, Nadi A, Alizadeh M, Rezakhani L. Exosome-loaded scaffolds for regenerative medicine in hard tissues. *Tissue Cell.* 2023;82:102102. doi:10.1016/j.tice.2023.102102
18. Chung IM, Rajakumar G, Venkidasamy B, Subramanian U, Thiruvengadam M. Exosomes: current use and future applications. *Clinica Chimica Acta.* 2020;500:226–232. doi:10.1016/j.cca.2019.10.022
19. Liao W, Du Y, Zhang C, et al. Exosomes: the next generation of endogenous nanomaterials for advanced drug delivery and therapy. *Acta Biomater.* 2019;86:1–14. doi:10.1016/j.actbio.2018.12.045
20. Hu L, Wang J, Zhou X, et al. Exosomes derived from human adipose mesenchymal stem cells accelerates cutaneous wound healing via optimizing the characteristics of fibroblasts. *Sci Rep.* 2016;6:32993. doi:10.1038/srep32993
21. Zhang W, Wang L, Guo H, Chen L, Huang X. Dapagliflozin-loaded exosome mimetics facilitate diabetic wound healing by HIF-1 $\alpha$ -mediated enhancement of angiogenesis. *Adv Healthcare Mater.* 2023;12(7):e2202751.
22. Kim H, Wang SY, Kwak G, Yang Y, Kwon IC, Kim SH. Exosome-guided phenotypic switch of M1 to M2 macrophages for cutaneous wound healing. *Adv Sci.* 2019;6(20):1900513. doi:10.1002/adv.201900513
23. Wang J, Yi Y, Zhu Y, et al. [Effects of adipose-derived stem cell released exosomes on wound healing in diabetic mice]脂肪干细胞来源外泌体促进糖尿病小鼠创面愈合的实验研究. *Zhongguo xiu fu chong jian wai ke za zhi* 《中国修复重建外科杂志》. 2020;34(1):124–131. Chinese. doi:10.7507/1002-1892.201903058
24. Dostert C, Grusdat M, Letellier E, Brenner D. The TNF family of ligands and receptors: communication modules in the immune system and beyond. *Physiol Rev.* 2019;99(1):115–160. doi:10.1152/physrev.00045.2017
25. Funk LH, Hackett AR, Bunge MB, Lee JK. Tumor necrosis factor superfamily member April contributes to fibrotic scar formation after spinal cord injury. *J Neuroinflamm.* 2016;13(1):87. doi:10.1186/s12974-016-0552-4
26. Noonan DM, Fulle A, Valente P, et al. The complete sequence of perlecan, a basement membrane heparan sulfate proteoglycan, reveals extensive similarity with laminin A chain, low density lipoprotein-receptor, and the neural cell adhesion molecule. *J Biol Chem.* 1991;266(34):22939–22947. doi:10.1016/S0021-9258(18)54445-8
27. Purushothaman A, Bandari SK, Liu J, Mobley JA, Brown EE, Sanderson RD. Fibronectin on the surface of myeloma cell-derived exosomes mediates exosome-cell interactions. *J Biol Chem.* 2016;291(4):1652–1663. doi:10.1074/jbc.M115.686295
28. Baiocchi A, Montaldo C, Conigliaro A, et al. Extracellular matrix molecular remodeling in human liver fibrosis evolution. *PLoS One.* 2016;11(3): e0151736. doi:10.1371/journal.pone.0151736
29. Warren CR, Grindel BJ, Francis L, Carson DD, Farach-Carson MC. Transcriptional activation by NF $\kappa$ B increases perlecan/HSPG2 expression in the desmoplastic prostate tumor microenvironment. *J Cell Biochem.* 2014;115(7):1322–1333. doi:10.1002/jcb.24788
30. Shu C, Smith SM, Melrose J. The heparan sulphate deficient Hspg2 exon 3 null mouse displays reduced deposition of TGF- $\beta$ 1 in skin compared to C57BL/6 wild type mice. *J Mol Histol.* 2016;47(3):365–374. doi:10.1007/s10735-016-9677-0
31. Tsiantoulas D, Eslami M, Obermayer G, et al. April limits atherosclerosis by binding to heparan sulfate proteoglycans. *Nature.* 2021;597(7874):92–96. doi:10.1038/s41586-021-03818-3
32. Zhao W, Zhang R, Zang C, et al. Exosome derived from mesenchymal stem cells alleviates pathological scars by inhibiting the proliferation, migration and protein expression of fibroblasts via delivering miR-138-5p to target SIRT1. *Int J Nanomedicine.* 2022;17:4023–4038. doi:10.2147/IJN.S377317
33. Yan D, Zhao H, Li C, et al. A clinical study of carbon dioxide lattice laser-assisted or microneedle-assisted 5-aminolevulinic acid-based photodynamic therapy for the treatment of hypertrophic acne scars. *Photodermatol Photoimmunol Photomed.* 2022;38(1):53–59. doi:10.1111/phpp.12716
34. Zhang K, Garner W, Cohen L, Rodriguez J, Phan S. Increased types I and III collagen and transforming growth factor-beta 1 mRNA and protein in hypertrophic burn scar. *J Invest Dermatol.* 1995;104(5):750–754. doi:10.1111/1523-1747.ep12606979
35. Ogawa R. Keloid and hypertrophic scars are the result of chronic inflammation in the reticular dermis. *Int J Mol Sci.* 2017;18(3):606. doi:10.3390/ijms18030606
36. Ogawa R, Akita S, Akaishi S, et al. Diagnosis and treatment of Keloids And Hypertrophic Scars-Japan Scar Workshop Consensus Document 2018. *Burns Trauma.* 2019;7:39. doi:10.1186/s41038-019-0175-y
37. Steele H, Cheng J, Willicut A, et al. TNF superfamily control of tissue remodeling and fibrosis. *Front Immunol.* 2023;14:1219907. doi:10.3389/fimmu.2023.1219907
38. Qian Z, Qingshan C, Chun J, et al. High expression of TNFSF13 in tumor cells and fibroblasts is associated with poor prognosis in non-small cell lung cancer. *Am J Clin Pathol.* 2014;141(2):226–233. doi:10.1309/AJCP4JP8BZOMHEAW
39. Zhou Z, Wang J, Cao R, et al. Impaired angiogenesis, delayed wound healing and retarded tumor growth in perlecan heparan sulfate-deficient mice. *Cancer Res.* 2004;64(14):4699–4702. doi:10.1158/0008-5472.CAN-04-0810
40. Chen Y, Shi-Wen X, van Beek J, et al. Matrix contraction by dermal fibroblasts requires transforming growth factor-beta/activin-linked kinase 5, heparan sulfate-containing proteoglycans, and MEK/ERK: insights into pathological scarring in chronic fibrotic disease. *Am J Pathol.* 2005;167(6):1699–1711. doi:10.1016/S0002-9440(10)61252-7
41. Hoffmann A, Baltimore D. Circuitry of nuclear factor kappaB signaling. *Immunol Rev.* 2006;210(1):171–186. doi:10.1111/j.0105-2896.2006.00375.x
42. Vallabhapurapu S, Karin M. Regulation and function of NF-kappaB transcription factors in the immune system. *Annu Rev Immunol.* 2009;27(1):693–733. doi:10.1146/annurev.immunol.021908.132641
43. Park SR, Kim PH, Lee KS, et al. April stimulates NF- $\kappa$ B-mediated HoxC4 induction for AID expression in mouse B cells. *Cytokine.* 2013;61(2):608–613. doi:10.1016/j.cyt.2012.10.018

44. Stephenson S, Care MA, Doody GM, Tooze RM. April drives a coordinated but diverse response as a foundation for plasma cell longevity. *J Immunol.* **2022**;209(5):926–937. doi:10.4049/jimmunol.2100623
45. Cornelis R, Hahne S, Taddeo A, et al. Stromal cell-contact dependent PI3K and April induced NF- $\kappa$ B signaling prevent mitochondrial- and ER stress induced death of memory plasma cells. *Cell Rep.* **2020**;32(5):107982. doi:10.1016/j.celrep.2020.107982
46. Hao S, Baltimore D. The stability of mRNA influences the temporal order of the induction of genes encoding inflammatory molecules. *Nature Immunol.* **2009**;10(3):281–288. doi:10.1038/ni.1699
47. Zhang L, Xiang J, Zhang F, Liu L, Hu C. MSCs can be a double-edged sword in tumorigenesis. *Front Oncol.* **2022**;12:1047907. doi:10.3389/fonc.2022.1047907
48. Kim KS, Kim HS, Park JM, et al. Long-term immunomodulatory effect of amniotic stem cells in an Alzheimer's disease model. *Neurobiol Aging.* **2013**;34(10):2408–2420. doi:10.1016/j.neurobiolaging.2013.03.029
49. Yuan T, Meijia L, Xinyao C, Xinyue C, Lijun H. Exosome derived from human adipose-derived stem cell improve wound healing quality: a systematic review and meta-analysis of preclinical animal studies. *Int Wound J.* **2023**;20(6):2424–2439. doi:10.1111/iwj.14081
50. Rezakhani L, Alizadeh M, Sharifi E, Soleimannejad M, Alizadeh A. Isolation and characterization of crab haemolymph exosomes and its effects on Breast Cancer Cells (4T1). *Cell J.* **2021**;23(6):658–664. doi:10.22074/cellj.2021.7595
51. Rashidi M, Bijari S, Khazaei AH, Shojaei-Ghahrizjani F, Rezakhani L. The role of milk-derived exosomes in the treatment of diseases. *Front Genetics.* **2022**;13:1009338. doi:10.3389/fgene.2022.1009338
52. Ding J, Wang X, Chen B, Zhang J, Xu J. Exosomes derived from human bone marrow mesenchymal stem cells stimulated by deferroxamine accelerate cutaneous wound healing by promoting angiogenesis. *Biomed Res Int.* **2019**;2019:9742765. doi:10.1155/2019/9742765

## International Journal of Nanomedicine

Dovepress

### Publish your work in this journal

The International Journal of Nanomedicine is an international, peer-reviewed journal focusing on the application of nanotechnology in diagnostics, therapeutics, and drug delivery systems throughout the biomedical field. This journal is indexed on PubMed Central, MedLine, CAS, SciSearch®, Current Contents®/Clinical Medicine, Journal Citation Reports/Science Edition, EMBase, Scopus and the Elsevier Bibliographic databases. The manuscript management system is completely online and includes a very quick and fair peer-review system, which is all easy to use. Visit <http://www.dovepress.com/testimonials.php> to read real quotes from published authors.

Submit your manuscript here: <https://www.dovepress.com/international-journal-of-nanomedicine-journal>